
Article:
Kulmaczewski, R orcid.org/0000-0002-3855-4530, Cespedes, O orcid.org/0000-0002-5249-9523 and Halcrow, MA orcid.org/0000-0001-7491-9034 (2017) Gradual thermal spin-crossover mediated by a reentrant Z' = 1 → Z' = 6 → Z' = 1 phase transition. Inorganic Chemistry, 56 (6). pp. 3144-3148. ISSN 0020-1669

https://doi.org/10.1021/acs.inorgchem.7b00071

Gradual Thermal Spin-Crossover Mediated by a Re-Entrant $Z' = 1 \rightarrow Z' = 6 \rightarrow Z' = 1$ Phase Transition

Rafal Kulmaczewski[†], Oscar Cespedes[‡] and Malcolm A. Halcrow*[,†].

[†]School of Chemistry, University of Leeds, Woodhouse Lane, Leeds LS2 9JT, UK.

[‡]School of Physics and Astronomy, University of Leeds, E. C. Stoner Building, Leeds LS2 9JT, UK.

ABSTRACT: The $Fe[BF_4]_2$ complex of the Schiff base podand *tris*-(4-{thiazol-4-yl}-3-aza-3-butenyl)amine exhibits gradual thermal spin-crossover with $T_{½} \approx 208$ K in the solid state. A weak discontinuity in the magnetic susceptibility curve at 190 K is associated with a re-entrant symmetry breaking transition involving a trebling of the unit cell volume (from $P2_1/c$, $Z = 4$ to $P2_1$, $Z = 12$). The intermediate phase contains six independent cations in puckered layers of low-spin, and high-spin or mixed-spin, molecules with an overall 30 % high-spin population at 175 K.

Spin-crossover compounds undergo a reversible transition between high-spin and low-spin electronic states under the influence of temperature or other physical stimuli.[1,2] This can lead to changes in the color, magnetic moment,[3] conductivity,[4] dielectric constant[5] and/or fluorescence[6] of a material, as well as inducing a mechanical response.[7] Spin-crossover transitions function in particles[1,8] or thin films[1,9] at the nanoscale, and have also been detected in single molecule junctions.[10] The structural chemistry of molecular spin-crossover materials continues to be widely studied because of this functional flexibility.[1,2] Thermal spin-transitions in bulk phases can exhibit varying degrees of cooperativity, occurring gradually or abruptly; with or without hysteresis; completely or incompletely; and, continuously (in one step) or discontinuously (in two or more steps).[11] Crystal engineering of spin-crossover compounds is a fundamental challenge, for the design of new materials for application purposes.[12]

Discontinuous spin-transitions can arise for a number of reasons.[12] In particular, single or re-entrant crystallographic phase changes between the spin states can perturb the progress of a spin-transition, often affording a plateau region over a finite temperature range with a mixed high:low-spin population.[13] Since the first discovery in $[Fe(pic)_3]Cl_2{\cdot}EtOH$ (pic = 2-{aminomethyl}-pyridine),[14] a variety of re-entrant symmetry-breaking phase behaviors have been found in different spin-crossover compounds.[15,16] The high- and low-spin molecules in the resultant intermediate phases are typically segregated into sub-lattices with 0D (checkerboard), 1D (chain) or 2D (layer) dimensionality.

Since crystallographic phase changes are cooperative phenomena, symmetry-breaking phase changes are usually associated with abrupt thermal spin-transitions.[13] However, we report here a new compound **1** (Chart 1) exhibiting re-entrant symmetry breaking that, unusually, is associated with a gradual thermal spin-crossover.[17]

Complex **1** was formed by reaction of a 3:1:1 ratio of thiazole-4-carboxaldehyde, *tris*-(2-aminoethyl)amine and $Fe[BF_4]_2{\cdot}6H_2O$ in refluxing ethanol. After the usual work-up, slow diffusion of diethyl ether vapor into nitromethane solutions of the compound yielded orange solvent-free crystals. Spin-crossover in **1** occurs gradually between the temperatures of 100-350 K, with $T_{½}$ = 208±2 K from magnetic susceptibility data. The spin-crossover proceeds without thermal hysteresis but has a small discontinuity near 190 K, just below $T_{½}$ (Figure 1).

Chart 1. Compound **1**.

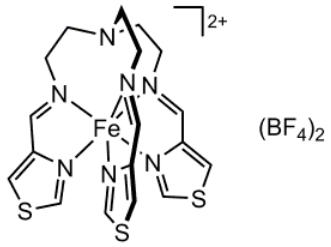

1

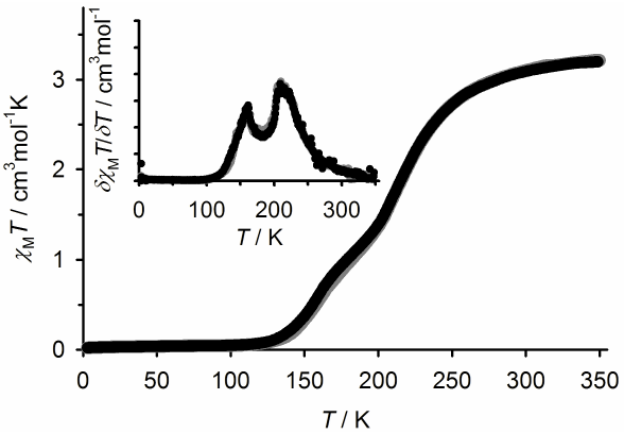

Figure 1 Variable temperature magnetic susceptibility data for polycrystalline **1**, at scan rate 5 $Kmin^{-1}$, on cooling (black) and warming (gray) temperature ramps. The inset graph shows the first derivative of the curves.

At first glance, crystals of **1** retain the same space group at all temperatures ($P2_1/c$, $Z = 4$). The unit cell contains one formula unit of the compound, with no crystallographically imposed symmetry. Although podand complexes like **1** have a helical ligand conformation (Figure S3),[18] **1** crystallizes as a racemate with equal numbers of Λ and Δ helical molecules in the centrosymmet-

ric crystal. Its unit cell volume decreases smoothly on cooling from 300 to 130 K, consistent with a gradual spin-crossover. However, this masks a discontinuous increase in *b* and a decrease in *c* between 150-200 K (Figures S1 and S2). That implies the spin-crossover discontinuity around 190 K in **1** is linked to a change in the thermal expansion properties of the crystal.

Five different crystals of **1** were examined, which were all isostructural at 300 and 120 K. The crystal reported here gave typical results, and was studied at seven temperatures within that range. The complex is essentially high-spin at 300 K and low-spin at 120 K according to its metric parameters. Structures at intermediate temperatures imply a mixed spin-state population, with a smooth high→low spin conversion upon cooling. This is accompanied by a conformational rearrangement of the podand ligand, such that the Fe…N distance to the non-coordinated bridgehead N atom is *ca* 0.7 Å longer in the low-spin state (Figure S3). That structure rearrangement is typical for spin-crossover in tren-based podand complexes.[12,17]

More unusually, the atomic displacement parameters in the complex molecule grow steadily larger and more elongated on cooling between 250-175 K, before slowly contracting again at lower temperatures. At 150 K, the Fourier map resolved two equally occupied disorder sites for the complete complex molecule, which were refined with distance restraints applied to the ligand atoms; additional disorder at one thiazolyl ring was also included (Figures S4 and S5). The same disorder model refined successfully at 175, 200 and 225 K, each with improved refinement residuals compared to the ordered cation model. However, refinements based on a single wholly occupied cation site were superior at the other temperatures examined. The whole-molecule disorder sites at each intermediate temperature have comparable spin-state populations (Figure 2). Hence the disorder orientations do not simply correspond to the high-spin and low-spin forms of the molecule, but are a reflection of the lattice dynamics.

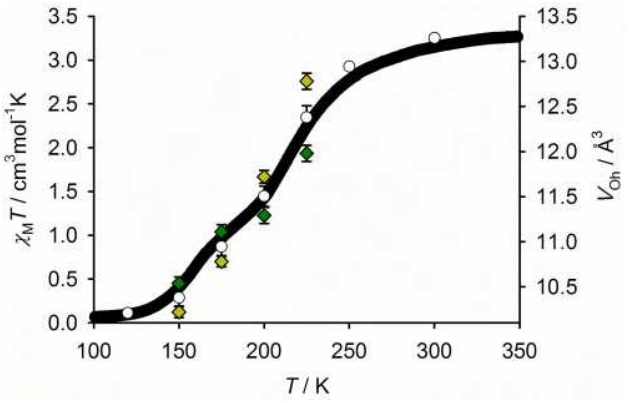

Figure 2 The evolution of the coordination sphere in the parent phase of **1** (V_{Oh}, white circles),[19] compared with the progress of the spin-crossover transition (black spheres; Figure 1). Between 150-225 K, V_{Oh} for the two molecular disorder sites is shown as green and yellow diamonds, and the white circles represent the average of the two.

The metric parameters from these crystallographic refinements reproduce the form of the gradual spin-crossover in **1** (Figures 2 and S7). While Figure 2 implies the cation disorder sites at intermediate temperatures may undergo spin-crossover at different rates, this should be interpreted with care because of the disordered nature of the crystal. None-the-less, the averaged V_{Oh} values from the partial cations agree excellently with the spin-crossover measured from magnetic data, including the inflection near 190 K (Figure 2).

Additional weak reflections were observed in the diffraction images from **1** around 175 K, where the molecular disorder is most pronounced (Figure S6). These data could sometimes be merged to a larger monoclinic supercell, whose volume is three times larger than the original unit cell. The dimensions of the supercell relate to the parent unit cell as follows: $a' = \sqrt{([3/2])}c$; $b' = b$; $c' = (\sqrt{6})a$; and $\beta' = \beta$.[20] That would be consistent with a re-entrant symmetry-breaking transformation to an intermediate crystal phase during the progress of the spin-crossover. While the extra diffraction peaks were consistently observed in different experiments, in most cases data merged to the supercell could only be solved and refined after transformation into the original, reduced $P2_1/c$ unit cell.[21] This was the case for experiments involving the crystal described above. However, a successful solution of the enlarged supercell at 175 K was obtained from one experiment using a different crystal. The refinement of the intermediate phase has relatively low precision, reflecting the size of the model and significant cation and anion disorder which was only partly resolvable. However, the basic features of the intermediate phase are clear (Figure 3).

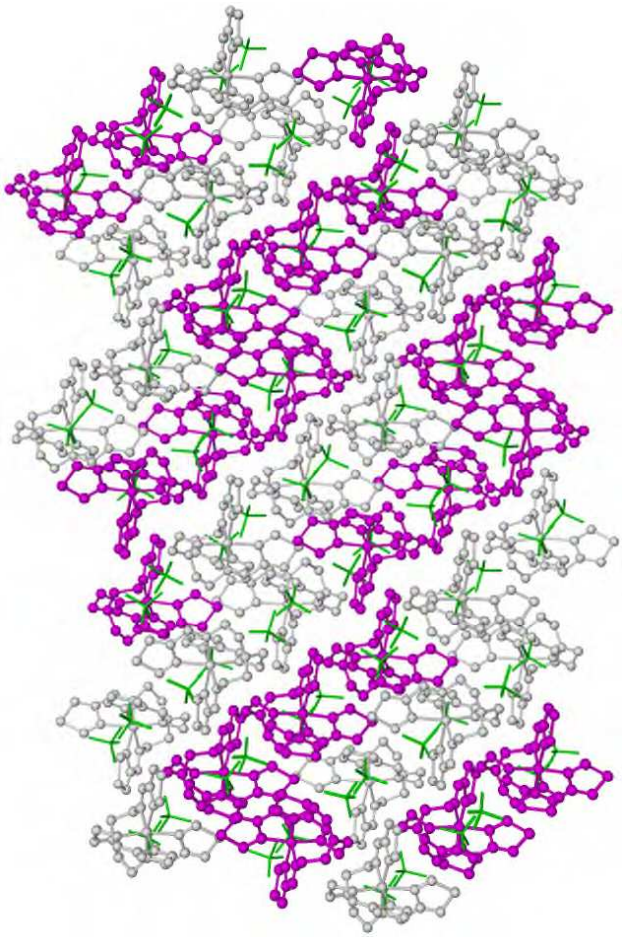

Figure 3 Packing diagram of the intermediate phase of **1**, showing the segregation of the low-spin (purple) and high-spin/mixed-spin (white) molecules into puckered layers in the lattice. Only one orientation of the disordered residues is shown, and the BF_4^- ions (green) are de-emphasized. The view shows the (010) lattice plane, with the *c* axis vertical.

The asymmetric unit of the intermediate phase ($P2_1$, Z = 12) contains six unique complex molecules, with molecules A, B and C in the model having a Δ helical ligand conformation molecules D, E and F a Λ conformation. The intermediate phase is also a perfect racemic twin, which is to be expected given the centrosymmetric nature of the parent phase. Based on their metric parameters three of the unique molecules are low-spin; one is predominantly high-spin; and the other two have a mixed high:low spin-state population (Table S4). That is consistent with the *ca* 30 % high-spin fraction predicted by the magnetic susceptibility curve at that temperature ($\chi_M T$ = 0.98 $cm^3mol^{-1}K$ at 175 K). It also agrees well with the structure refinement of the parent phase at the same temperature (Tables S3 and S4). The low-spin cations (molecules B, E and F in the refinement) and the high-spin/mixed spin cations (molecules A, C and D) are grouped into puckered, interdigitated layers running parallel to the (102) lattice plane (Figure 3). There is no correlation between the spin-state and ligand helicity in the different cations.

Important intermolecular contacts in the lattice of **1** are listed in Tables S5-S7. There is a typical distribution of weak intermolecular C–H…F and S…F contacts between the cations and anions in the low-spin form of **1**. However, there is no long-range network of direct interactions between the complex cations, to propagate a spin-transition through a lattice. Rather, just centrosymmetric pairs of molecules in **1** are in direct contact, through one unique C–H…S interaction that is 0.2 Å shorter than the van der Waals sum of those atoms at 120 K (Figure 4). There is also no π–π overlap between thiazolyl rings in neighboring molecules. The same is true for the intermediate phase, except that there are fewer of the short intermolecular C–H…S contacts between cations. Relief of that steric clash may be one of the drivers for the local disorder and formation of the intermediate phase during the spin-crossover process. The high-spin form of **1** has no short intermolecular C–H…X (X = F or S) contacts of any type at 300 K.[21] The relatively open crystal packing in **1** is illustrated by its crystal density. This is 4.3-4.4 % lower than an analogous podand complex with the same empirical formula, which exhibits a much more cooperative spin transition (Table S8).[17]

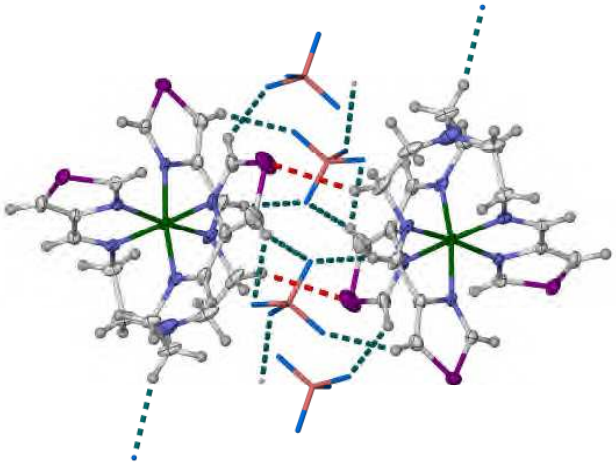

Figure 4 The short intemolecular C–H…X interactions in **1** at 120 K. Only one orientation of the disordered BF_4^- ion is shown for clarity. H…F interactions of < 2.5 Å are shown in green, while the C–H…S contacts between cations are highlighted in red. Color code: C, white; H, pale gray; B, pink; F, cyan; Fe, green; N, blue; S, purple.

Compared to other literature examples, the re-entrant Z' = 1 → Z' = 6 → Z' = 1 phase behavior of **1** is unusual for two reasons. First, is the number of independent molecules in the asymmetric unit of the intermediate phase, which is among the largest known in a spin-crossover crystal.[15] More fundamentally, the gradual nature of spin-crossover in **1** is also notable. As mentioned above, symmetry-breaking phase changes usually have a profound effect on a spin-transition, leading to abrupt, discontinuous and/or stepwise switching upon cooling.[13] However, the symmetry breaking transition in **1** has a negligible effect on the progress of its spin-crossover, and is barely reflected in the magnetic susceptibility data (Figures 1 and 3). The weakly cooperative nature of **1** is consistent with its low-density crystal packing (Table S8), where the cations are well-separated from each other by the BF_4^- anions.[12] That might explain the inconsistent resolution of the intermediate phase in different experiments. While significant rearrangement of the cations within their lattice sites between 150-225 K is evident from their crystallographic disorder (Figures S4 and S5), this rarely occurs with sufficient long-range order to be resolved in a single crystal dataset.

In conclusion, this study demonstrates that gradual spin-crossover transitions that are unexceptional at first glance can involve more complicated structural chemistry, that merits detailed characterization.

ASSOCIATED CONTENT

Supporting Information

Full experimental details, tables of metric parameters, additional crystallographic figures and variable temperature unit cell data. This material is available free of charge via the Internet at http://pubs.acs.org. CCDC 1519291–1519297 (parent phase) and 1526385 (intermediate phase) containing the supplementary crystallographic data can be obtained free of charge from the Cambridge Crystallographic Data Center via www.ccdc.cam.ac.uk/data_request/cif.

AUTHOR INFORMATION

Corresponding Author

*E-mail: m.a.halcrow@leeds.ac.uk.

ORCID

Malcolm Halcrow: 0000-0001-7491-9034

Author Contributions

All authors have given approval to the final version of the manuscript.

Notes

The authors declare no competing financial interests. Experimental data sets associated with this paper are available from the University of Leeds library (http://doi.org/10.5518/164).

ACKNOWLEDGMENT

This work was funded by the EPSRC (EP/K012568/1 and EP/K00512X/1).

REFERENCES

(1) *Spin-Crossover Materials–Properties and Applications*; Halcrow, M. A., Ed.; John Wiley & Sons, Ltd.: New York, 2013; p 568.

(2) (a) Gütlich, P. Spin Crossover – Quo Vadis? *Eur. J. Inorg. Chem.* **2013**, 581−591. (b) Gütlich, P.; Gaspar, A. B.; Garcia, Y. Spin State Switching in Iron Coordination Compounds. *Beilstein J. Org. Chem.* **2013**, *9*, 342−391. (c) Guionneau, P. Crystallography and Spin-Crossover. A View of Breathing Materials. *Dalton Trans.* **2014**, *43*, 382−393. (d)

Brooker, S. Spin Crossover with Thermal Hysteresis: Practicalities and Lessons Learnt. *Chem. Soc. Rev.* **2015**, *44*, 2880−2892.

(3) Kahn, O.; Kröber, J.; Jay, C. Spin Transition Molecular Materials for Displays and Data Recording. *Adv. Mater.* **1992**, *4*, 718–728.

(4) See eg (a) Matsuda, M.; Tajima, H. Thin Film of a Spin Crossover Complex $[Fe(dpp)_2](BF_4)_2$. *Chem. Lett.* **2007**, *36*, 700–701. (b) Takahashi, K.; Cui, H.-B.; Okano, Y.; Kobayashi, H.; Mori, H.; Tajima, H.; Einaga, Y; Sato, O. Evidence of the Chemical Uniaxial Strain Effect on Electrical Conductivity in the Spin-Crossover ConductingMolecular System: $[Fe^{III}(qnal)_2][Pd(dmit)_2]_5$·acetone. *J. Am. Chem. Soc.* **2008**, *130*, 6688–6689. (c) Rotaru, A.; Gural'skiy, I. A.; Molnár, G.; Salmon, L.; Demont, P.; Bousseksou, A. Spin State Dependence of Electrical Conductivity of Spin Crossover Materials. *Chem. Commun.* **2012**, *48*, 4163–4165. (d) Phan, H.; Benjamin, S. M.; Steven, E.; Brooks, J. S.; Shatruk, M. Photomagnetic Response in Highly Conductive Iron(II) Spin-Crossover Complexes with TCNQ Radicals. *Angew. Chem. Int. Ed.* **2015**, *54*, 823–827.

(5) See eg (a) Bonhommeau, S.; Guillon, T.; Daku, L. M. L.; Demont, P.; Costa, J. S.; Létard, J.-F.; Molnár, G.; Bousseksou, A. Photoswitching of the Dielectric Constant of the Spin-Crossover Complex $[Fe(L)(CN)_2]\cdot H_2O$. *Angew. Chem. Int. Ed.* **2006**, *45*, 1625–1629. (b) Bovo, G.; Bräunlich, I.; Caseri, W. R.; Stingelin, N.; Anthopoulos, T. D.; Sandeman, K. G.; Bradley, D. D. C.; Stavrinou, P. N. Room Temperature Dielectric Bistability in Solution-Processed Spin Crossover Polymer Thin Films. *J. Mater. Chem. C* **2016**, *4*, 6240–6248.

(6) See eg (a) Garcia, Y.; Robert, F.; Naik, A. D.; Zhou, G.; Tinant, B.; Robeyns, K.; Michotte, S.; Piraux, L. Spin Transition Charted in a Fluorophore-Tagged Thermochromic Dinuclear Iron(II) Complex. *J. Am. Chem. Soc.* **2011**, *133*, 15850–15853. (b) Titos-Padilla, S.; Herrera, J. M.; Chen, X.-W.; Delgado, J. J.; Colacio, E. Bifunctional Hybrid SiO2 Nanoparticles Showing Synergy between Core Spin Crossover and Shell Luminescence Properties. *Angew. Chem. Int. Ed.* **2011**, *50*, 3290−3293. (c) Wang, C.-F.; Li, R.-F.; Chen, X.-Y.; Wei, R.-J.; Zheng, L.-S.; Tao, J. Synergetic Spin Crossover and Fluorescence in One-Dimensional Hybrid Complexes. *Angew. Chem., Int. Ed.* **2015**, *54*, 1574–1577. (d) Herrera, J. M.; Titos-Padilla, S.; Pope, S. J. A.; Berlanga, I.; Zamora, F.; Delgado, J. J.; Kamenev, K. V.; Wang, X.; Prescimone, A.; Brechin, E. K.; Colacio, E. Studies on Bifunctional Fe(II)-Triazole Spin Crossover Nanoparticles: Time-Dependent Luminescence, Surface Grafting and the Effect of a Silica Shell and Hydrostatic Pressure on the Magnetic Properties. *J. Mater. Chem. C* **2015**, *3*, 7819–7829.

(7) Manrique-Juárez, M. D.; Rat, S.; Salmon, L.; Molnár, G.; Quintero, C. M.; Nicu, L.; Shepherd, H. J.; Bousseksou, A. Switchable Molecule-Based Materials for Micro- and Nanoscale Actuating Applications: Achievements and Prospects. *Coord. Chem. Rev.* **2016**, *308*, 395–408.

(8) (a) Catala, L.; Volatron, F.; Brinzei, D.; Mallah, T. Functional Coordination Nanoparticles. *Inorg. Chem.* **2009**, *48*, 3360−3370. (b) Roubeau, O. Triazole-Based One-Dimensional Spin-Crossover Coordination Polymers. *Chem. Eur. J.* **2012**, *18*, 15230–15244. (c) Mikolasek, M.; Félix, G.; Nicolazzi, W.; Molnár, G.; Salmon, L.; Bousseksou, A. Finite Size Effects in Molecular Spin Crossover Materials. *New J. Chem.* **2014**, *38*, 1834–1839. (d) Tissot, A. Photoswitchable Spin Crossover Nanoparticles. *New J. Chem.* **2014**, *38*, 1840–1845.

(9) (a) Cavallini, M. Status and Perspectives in Thin Films and Patterning of Spin Crossover Compounds. *Phys. Chem. Chem. Phys.* **2012**, *14*, 11867−11876. (b) Lefter, C.; Davesne, V.; Salmon, L.; Molnár, G.; Demont, P.; Rotaru, A.; Bousseksou, A. Charge Transport and Electrical Properties of Spin Crossover Materials: Towards Nanoelectronic and Spintronic Devices. *Magnetochemistry* **2016**, *2*, 18/1–19.

(10) (a) Harzmann, G. D.; Frisenda, R.; van der Zant, H. S. J.; Mayor, M. Single-Molecule Spin Switch Based on Voltage-Triggered Distortion of the Coordination Sphere. *Angew. Chem. Int. Ed.* **2015**, *54*, 13425−13430. (b) Aragonès, A. C.; Aravena, D.; Cerdá, J. I.; Acís-Castillo, Z.; Li, H.; Real, J. A.; Sanz, F.; Hihath, J.; Ruiz, E.; Díez-Pérez, I. Large Conductance Switching in a Single-Molecule Device through Room Temperature Spin-Dependent Transport. *Nano Lett.* **2016**, *16*, 218−226.

(11) Gütlich, P.; Hauser, A.; Spiering, H. Thermal and Optical Switching of Iron(II) Complexes. *Angew. Chem. Int. Ed.* **1994**, *33*, 2024–2054.

(12) Halcrow, M. A. Structure:Function Relationships in Molecular Spin-Crossover Complexes. *Chem. Soc. Rev.* **2011**, *40*, 4119−4142.

(13) (a) Shatruk, M.; Phan, H.; Chrisostomo, B. A.; Suleimenova, A. Symmetry-Breaking Structural Phase Transitions in Spin CrossoverComplexes. *Coord. Chem. Rev.* **2015**, *289–290*, 62–73. (b) Ortega-Villar, N.; Muñoz, M. C.; Real, J. A. Symmetry Breaking in Iron(II) Spin-Crossover Molecular Crystals. *Magnetochemistry* **2016**, *2*, 16/1–22.

(14) Chernyshov, D.; Hostettler, M.; Törnroos, K. M.; Bürgi, H.-B. Ordering Phenomena and Phase Transitions in a Spin-Crossover Compound – Uncovering the Nature of the Intermediate Phase of $[Fe(2\text{-pic})_3]Cl_2\cdot EtOH$. *Angew. Chem. Int. Ed.* **2003**, *42*, 3825–3830.

(15) (a) Brefuel, N.; Collet, E.; Watanabe, H.; Kojima, M.; Matsumoto, N.; Toupet, L.; Tanaka, K.; Tuchagues, J.-P. Nanoscale Self-Hosting of Molecular Spin-States in the Intermediate Phase of a Spin-Crossover Material. *Chem. Eur. J.* **2010**, *16*, 14060–14068. (b) Lennartson, A.; Bond, A. D.; Piligkos, S.; McKenzie, C. J. Four-Site Cooperative Spin Crossover in a Mononuclear Fe^{II} Complex. *Angew. Chem. Int. Ed.* **2012**, *51*, 11049–11052. (c) Murnaghan, K. D.; Carbonera, C.; Toupet, L.; Griffin, M.; Dîrtu, M. M.; Desplanches, C.; Garcia, Y.; Collet, E.; Létard, J.-F.; Morgan, G. G. Spin-State Ordering on One Sub-lattice of a Mononuclear Iron(III) Spin Crossover Complex Exhibiting LIESST and TIESST. *Chem. Eur. J.* **2014**, *20*, 5613–5618.

(16) See *eg* (a) Money, V. A.; Carbonera, C.; Elhaïk, J.; Halcrow, M. A.; Howard, J. A. K.; Létard, J.-F. Interplay Between Kinetically Slow Thermal Spin-Crossover and Metastable High-Spin State Relaxation in an Iron(II) Complex with Similar $T_{½}$ and T(LIESST). *Chem. Eur. J.* **2007**, *13*, 5503−5514. (b) Bonnet, S.; Siegler, M. A.; Costa, J. S.; Molnár, G.; Bousseksou, A.; Spek, A. L.; Gamez. P.; Reedijk, J. A Two-Step Spin Crossover Mononuclear Iron(II) Complex with a [HS–LS–LS] Intermediate Phase. *Chem. Commun.* **2008**, 5619–5621. (c) Kusz, J,; Nowak, M.; Gütlich, P. Crystal-Structure Studies of Mononuclear Iron(II) Complexes with Two-Step Spin Crossover: [Fe{5-NO_2-sal-N(1,4,7,10)}] Revisited. *Eur. J. Inorg. Chem.* **2013**, 832–842. (d) Li, Z.-Y.; Dai, J.-W.; Shiota, Y.; Yoshizawa, K.; Kanegawa, S.; Sato, O. Multi-Step Spin Crossover Accompanied by Symmetry Breaking in an Fe^{III} Complex: Crystallographic Evidence and DFT Studies. *Chem. Eur. J.* **2013**, *19*, 12948–12952. (e) Vieira, B. J. C.; Coutinho, J. T.; Santos, I. C.; Pereira, L. C. J.; Waerenborgh, J. C.; da Gama, V. [Fe(nsal$_2$trien)]SCN, a New Two-Step Iron(III) Spin Crossover Compound, with Symmetry Breaking Spin-State Transition and an Intermediate Ordered State. *Inorg. Chem.* **2013**, *52*, 3845−3850.

(17) Another iron(II)/*tris*-thiazolyl podand complex, that is an isomer of **1** and also exhibits spin-crossover, has recently been reported. Struch, N.; Wagner, N.; Schnakenburg, G.; Weisbarth, R.; Klos, S.; Beck, J.; Lützen, A. Thiazolylimines as Novel Ligand-Systems for Spin-Crossover Centred Near Room Temperature. *Dalton Trans.* **2016**, *45*, 14023–14029.

(18) See *eg* (a) Katsuki, I.; Motoda, Y.; Sunatsuki, Y.; Matsumoto, N.; Nakashima, T.; Kojima, M. Spontaneous Resolution Induced by Self-Organization of Chiral Self-Complementary Cobalt(III) Complexes with Achiral Tripod-Type Ligands Containing Three Imidazole Group. *J. Am. Chem. Soc.* **2002**, *124*, 629–640. (b) Lazar, H. Z.; Forestier, T.; Barrett, S. A.; Kilner, C. A.; Létard, J.-F.; Halcrow, M. A. Thermal and Light-Induced Spin-Crossover in Salts of the Heptadentate Complex [*Tris*(4-{pyrazol-3-yl}-3-aza-3-butenyl)amine]iron(II). *Dalton Trans.* **2007**, 4276–4285. (c) McDaniel, A. M.; Klug, C. M.; Shores, M. P. Synthesis of Functionalized Hexadentate Iminopyridine Fe^{II} Complexes – Toward Anion-Dependent Spin Switching in Polar Media. *Eur. J. Inorg. Chem.* **2013**, 943–950.

(19) V_{Oh} is the volume of the FeN_6 coordination octahedron in the complex molecule, which is typically *ca* 10 Å^3 in the low-spin state and 13 Å^3 in high-spin state of iron(II) complexes. Guionneau, P.; Marchivie, M.; Bravic, G.; Létard, J.-F.; Chasseau, D. Structural Aspects of Spin Crossover. Example of the $[Fe^{II}L_n(NCS)_2]$ Complexes. *Top. Curr. Chem.* **2004**, 2*34*, 97−128.

(20) Typical dimensions of the re-entrant supercell of **1** at 175 K: a = 15.3548(7), b = 17.7741(8), c = 29.6348(14) Å, β = 102.952(5)°, V = 7882.1(6) Å^3. The reduced, parent unit cell from the same crystal at the same temperature is a = 12.0973(3), b = 17.7784(5), c = 12.5249(3) Å, β = 102.900(2)°, V = 2625.75(12) Å^3.

(21) Spek, A. L. Single-Crystal Structure Validation with the Program *PLATON*. *J. Appl. Crystallogr.* **2003**, *36*, 7−13.